JOURNAL OF COMPUTATIONAL PHYSICS **10**, 272–283 (1972)

Numerical Solution of the Glow Curve Differential Equations

D. SHENKER AND R. CHEN

Department of Physics and Astronomy, Tel-Aviv University, Tel-Aviv, Israel

Received July 1, 1971

The three basic simultaneous differential equations describing the phenomena of thermoluminescence and thermally stimulated conductivity are solved numerically for any given set of trapping parameters and without any additional assumptions, thus enabling us to simulate the TL and TSC phenomena.

The method employs a change of variable by which the high sensitivity of the solution to small numerical errors is overcome. Use is then made of an improved Runge–Kutta method for the solution of the new set of differential equations. Previous methods for extracting information from glow curves are tested using these calculated curves as data. The often used assumption $|\dot{n}_c| \ll |\dot{n}|, |\dot{m}|$ is explored and found to be correct for most of the temperature range of interest.

INTRODUCTION

The model explaining the appearance of a single thermoluminescence (TL) glow peak and its corresponding thermally stimulated conductivity (TSC) peak was represented mathematically by Halperin and Braner [1] by a set of three linear simultaneous equation as follows:

$$-dm/dt = Amn_c\,, \tag{1}$$

$$-dn/dt = P_0 n \exp(-E/kT) - B(N-n)\,n_c\,, \tag{2}$$

$$dn_c/dt = dm/dt - dn/dt, \tag{3}$$

where N is the concentration of traps (cm^{-3}); m is the concentration of holes (electrons) in recombination centers (cm^{-3}); n, the concentration of electrons (holes) in traps (cm^{-3}); n_c concentration of free electrons (holes) in the conduction (valence) band (cm^{-3}); t, the time; A and B, recombination and retrapping probabilities ($cm^3\,sec^{-1}$), respectively; P_0, the pre-exponential (frequency) factor (sec^{-1}); E, the activation energy (eV); k, the Boltzmann constant (eV/K); and T, the absolute temperature (K).

The luminescence intensity is given by $I = -\alpha(dm/dt)$ where α is a constant and the TSC by $\sigma = e\mu n_c$ where σ is the electrical conductivity; μ, the mobility

of free carriers; and e, the absolute value of the electron charge. The heating function $T = T(t)$ can be chosen at will. The phosphorescence decay can be considered as a special case for $T = \text{const}$. In many other cases the linear heating function $T = T_0 + \beta t$ is considered, for which the heating rate $dT/dt = \beta$ is constant.

This set of equations has previously been solved numerically [2–6] by assuming that

$$| dn_c/dt | \ll | dn/dt |, \qquad n_c \ll n, \tag{4}$$

assumptions that seem reasonable in many cases. It is, however, of interest to solve the equations without these simplifying assumptions. By doing so we can, among other things, test the validity of the above-mentioned assumptions (4). It is to be mentioned that this set of equations has previously been solved [7] for the special case of short time phosphorescence without the limiting conditions (4).

Approach to the Problem

Equations (1–3) are not adaptable for numerical solution in the original form since $| dm/dt | \approx | dn/dt | \gg | dn_c/dt |$ in most cases. A small relative error in Eqs. (1)–(2) would cause a large error in dn_c/dt; thus the solution tends to "blow up" after a certain time. The same problem arises in any transformation of the equations, in which at least one of the derivatives is computed by the multiplication of n_c, while n_c is computed directly from m and n.

We have overcome this difficulty by defining a new integration variable

$$x(t) = \int_{t_0}^{t} n_c \, dt, \tag{5}$$

where t is the time having initial value t_0. For any y which is a function of time we denote dy/dt by $\dot{y}$, dy/dx by y' and $y(t_i)$ by y_i. From Eq. (5) we get

$$\dot{y} = y'(dx/dt) = y'n_c . \tag{6}$$

From Eqs. (1)–(2) and (6) we get a set of three linear differential equations with the independent variable x and the dependent variables t, m and n as follows:

$$m' = -Am, \tag{7}$$

$$n' = -P_0(n/n_c) \exp(-E/kT) + B(N - n), \tag{8}$$

$$t' = 1/n_c . \tag{9}$$

In the simple case of a linear heating rate, T is given by $T = T_0 + \beta t$; for any other case we assume that $T = T(t)$ is some known function. n_c is computed separately in such a way as will cause minimal error in its value with the aid of Eq. (3) as explained further. Equation (7) is independent of Eqs. (8) and (9) and can therefore be solved directly;

$$m = m_0 \exp(-Ax), \tag{10}$$

where m_0 is the initial concentration of carriers in centers. Equations (8) and (9) therefore constitute a set of two coupled linear differential equations which are to be solved.

The Numerical Method

As usual, the numerical solution of differential equations requires the computation of the derivatives (in our case, n_i' and t_i') for given values of the variables (x_i , t_i , n_i), in each step i of the integration. We consider the case where A, B, P_0 , N and β are constants and the initial conditions m_0 , n_0 , n_{c_0} and T_0 (at t_0) are known. The initial values n_0' and t_0' are computed from Eqs. (8) and (9).

The first step of the solution (x_1) assumes that we are in the initial rise region; therefore we have

$$\dot{m}_1 = [-Am_0 n_{c_0} \exp(E/kT_0)] \exp(-E/kT_1), \tag{11}$$

and

$$n_{c1} = -\dot{m}_1/(Am_1) = (m_0 n_{c_0}/m_1) \exp(E/kT_0 - E/kT_1), \tag{12}$$

where m_1 is computed from Eq. (10). The insertion of n_{c1} in Eqs. (8) and (9) produces values for n_1' and t_1'. In the first step (and only there) we thus use the initial-rise assumption instead of Eq. (3) for evaluating the derivatives. We note that this assumption does not restrict the solution, as it holds true for low enough T_0 in any insulating or semiconducting crystal.

For $i \geqslant 2$, past values of $\ln(m_j)$ and t_j (for $j < i$) are used to fit a second order polynomial $\ln(m) = at^2 + bt + c$ through the three points $\ln(m_k)$, t_k for $k = i$, $i - 1$, $i - 2$. n_{ci}' is given by

$$n_{ci}' = \dot{n}_{ci}/n_{ci} = -(1/A)(d^2/dt^2)[\ln(m_i)]/\{-(1/A)(d/dt)[\ln(m_i)]\} = 2a/(b + 2at_i) \tag{13}$$

From Eq. (3) we get

$$n_i' = (\dot{m}_i - \dot{n}_{ci})/n_{ci} = -Am_i - n_{ci}' \tag{14}$$

so that n_{ci} can now be computed from Eq. (8):

$$n_{ci} = n_i P_0 \exp(-E/kT_i)/[B(N - n_i) - n_i']. \tag{15}$$

t_i is thus computed from Eq. (9).

The computation of n_i' and n_{ci} by Eqs. (13)–(15) ensures small errors in these variables. If $|(d^2/dt^2)(\ln m_i)|$ is small, large numerical errors may result in n'_{ci} [Eq. (13)]. On the other hand Am_i (which is relatively accurate) is much larger than n'_{ci} [Eq. (14)]; thus n_i' and therefore n_{ci} would be more accurate. If $|(d^2/dt^2)(\ln m_i)|$ is large, n'_{ci} would also be more accurate [Eq. (13)]; thus n_i' (and n_{ci}) would be accurate even when $| n'_{ci} | > Am_i$. A difficulty may arise only when m_i and $| \dot{m}_i |$ are very small, in which case Am_i and $d^2/dt^2(\ln m_i)$ become small. Fortunately this can happen only at the end of the decay of the TL curve and does not prevent the computation of the TL peak.

The computer program written for solving Eqs. (7)–(9) uses an improved Runge–Kutta method for the solution of simultaneous linear differential equations [8]. One starts by choosing a set of the parameters A, B, P_0, N and β and the initial values m_0, n_0, n_{c0} and T_0. The computed results t_i, m_i, n_i, n_{ci}, $\dot{m}_i$, $\dot{n}_i$ and $\dot{n}_{ci}$ are printed out and thus graphs of $| \dot{m} |$ (to which the TL intensity is proportional) and n_c as functions of t are plotted. The computation intervals are defined through the variable x and therefore are not constant in time (i.e., $t_i - t_{i-1}$ not necessarily equal to $t_{i+1} - t_i$). In ranges where n_{ci} increases during the process, the time intervals decrease [see Eq. (7)]. In order to avoid contraction of the time intervals, the maximal allowed step in the integration variable x is doubled when $t_i - t_{i-1}$ becomes smaller than 0.01 sec. Of course, $t_i - t_{i-1}$ depends on the choice of parameters and initial values, since t_i is solved from the differential equations.

Equations (7)–(9) can easily be solved as well for a nonconstant heating rate $[T = T(t)]$ or with parameters which vary with temperature by inserting as data the values of the parameters as functions of temperature. Phosphorescence curves can be otained by taking $\beta = 0$.

The computation usually ends when the final value of t, a priori chosen, is reached. Sometimes, due to numerical errors (usually when m or n become very small) the run has to be stopped before t final is reached.

The program was extended to solve a system of equations including several traps and recombination centers (assuming that the transitions into the recombination centers are solely from the conduction band). The set of differential equations is now

$$dm_i/dt = -n_c A_i m_i, \qquad i = 1,..., P, \tag{16}$$

$$dn_j/dt = -P_{0j} n_j \exp(-E_j/kT) + n_c B_j (N_j - n_j), \qquad j = 1,..., q, \tag{17}$$

$$dn_c/dt = \sum_{i=1}^{P} dm_i/dt - \sum_{j=1}^{q} dn_j/dt. \tag{18}$$

The solution is similarly obtained by using the new integration variable x given by (5).

Results and Discussion

Several solutions, corresponding to different sets of parameters and initial values were computed. These solutions made it possible to investigate quantitatively a number of assumptions usually made in glow curves analysis.

Figure 1 shows the solutions $| \dot{m} |$ and n_c as functions of temperature where the conditions are such that first order TL and TSC (n_c) peaks are found. In this

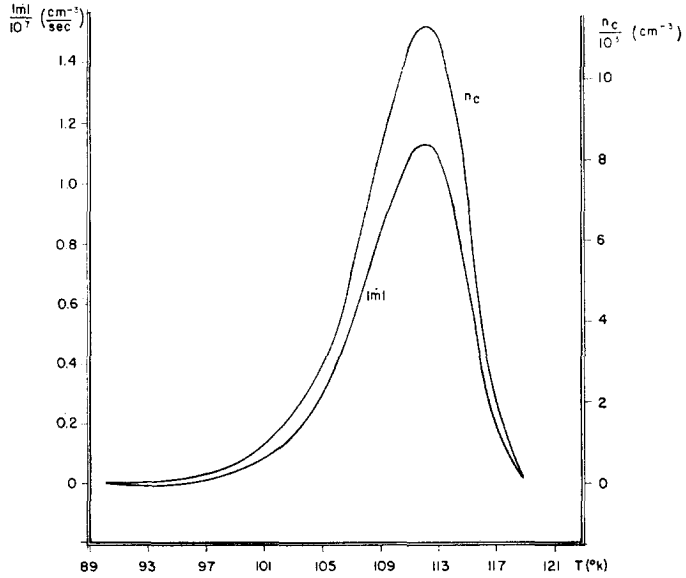

FIG. 1. Calculated peaks of n_c and $| \dot{m} |$ vs. temperature. $A = B = 10^{-7}$ cm^3 sec^{-1}, $P_0 = 10^{14}$ sec^{-1}, $E = 0.316$ ev, $m_0 = N = 10^{10}$ cm^{-3}, $n_0 = 10^8$ cm^{-3}, $\beta = 1K$/sec, $n_{c0} = 10$ cm^{-3}, $T_0 = 90$°K.

case the chosen recombination and retrapping probabilities A and B are the same whereas m_0 is larger than n_0 by two orders of magnitude. It is to be noted that this case is not the "classical" first order case where recombination is the dominating process as compared to retrapping. In this case, the recombination rate Am and the retrapping rate $B(N - n)$ are about the same in all the temperature range, yet the geometrical factor $\mu_g = \delta/\omega$ is 0.418, where $\delta = T_2 - T_m$ and $\omega = T_2 - T_1$ and where T_m is the temperature at the maximum intensity, and T_1 and T_2 the low and high temperatures at half intensity, respectively. In the

present case, the curves of n_c and $|\dot{m}|$ have the same shape, thus the μ_g value is the same for both. This value of ≈ 0.42 is characteristic of first order peaks [9]. Apart from the fact that a first order peak was thus found by the numerical solution of the differential equations without any additional assumption, the occurrence of first order peak can also be explained as follows. Assuming that $|\dot{n}_c| \ll |\dot{n}|$ and $n_c \ll n$, it was found [1] that

$$I = sn \exp(-E/kT) \frac{Am}{Am + B(N-n)} . \tag{19}$$

The term $Am/(Am + B(N-n))$ is reduced to unity when $Am \gg B(N-n)$, thus yielding the usual first-order equation. In the present case, however, this term is very close to being a constant as well, although its value is $\frac{1}{2}$; thus the first order peak results. Another important characteristic of the present case is that both the n_c and $|\dot{m}|$ peaks have exactly the same shape.

Figure 2 shows the TL and n_c peaks where $A = B$ and $m_0 = n_0$. The TL peak is of second order kinetics, which is characterized by $\mu_g = 0.525$ [9]. Another feature of these curves is that the maximum of the TL peak appears at a lower temperature than the corresponding maximum of the n_c curve. This effect has already been proved generally [10]. Thus, in principle this shift should have appeared in Fig. 1 as well, but the effect can be shown to be negligibly small

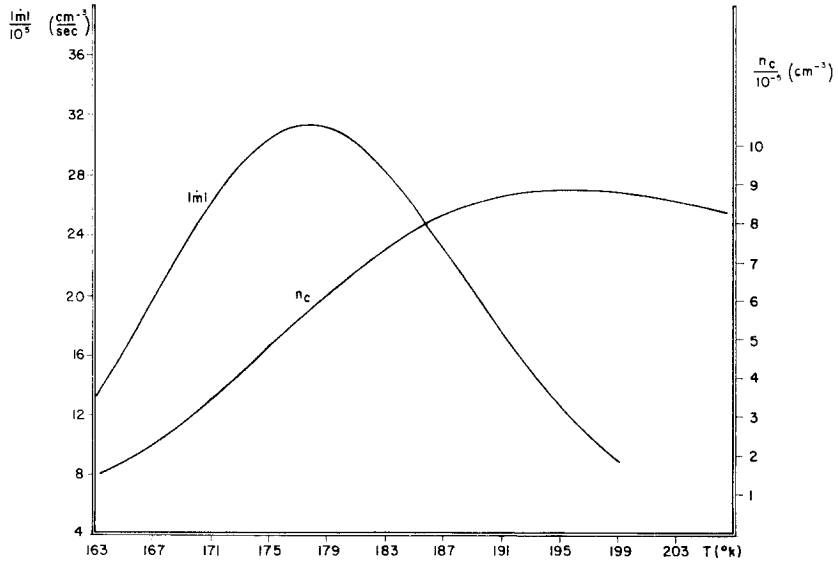

FIG. 2. Calculated peaks of n_c and $|\dot{m}|$. $A = B = 10^{-7}$ cm^3 sec^{-1}, $m_0 = n_0 = 10^8$ cm^{-3}, $N = 10^{10}$ cm^{-3}, $P_0 = 10^{10}$ sec^{-1}, $E = 0.316$ev, $\beta = 1K$/sec, $n_{c0} = 4 \times 10^3$ cm^{-3}, $T_0 = 140K$.

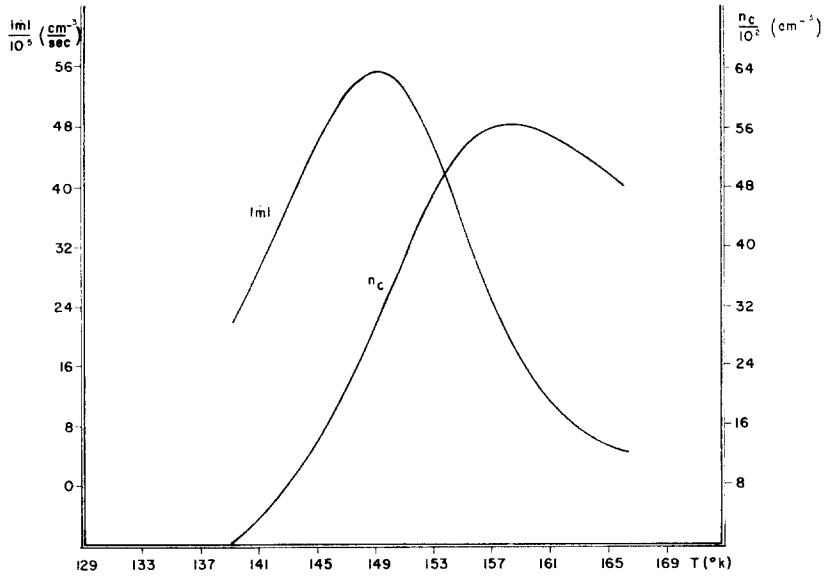

FIG. 3. Calculated peaks of n_c and $|\dot{m}|$. $A = 3 \times 10^{-5}$ cm^3 sec^{-1}, $B = 10^{-7}$ cm^3 sec^{-1}, $m_0 = n_0 = 10^8$ cm^{-3}, $N = 10^{10}$ cm^{-3}, $P_0 = 10^{10}$ sec^{-1}, $E = 0.316$ev, $\beta = 1K$/sec, $n_{c0} = 0.8$ cm^{-3}, $T_0 = 110K$.

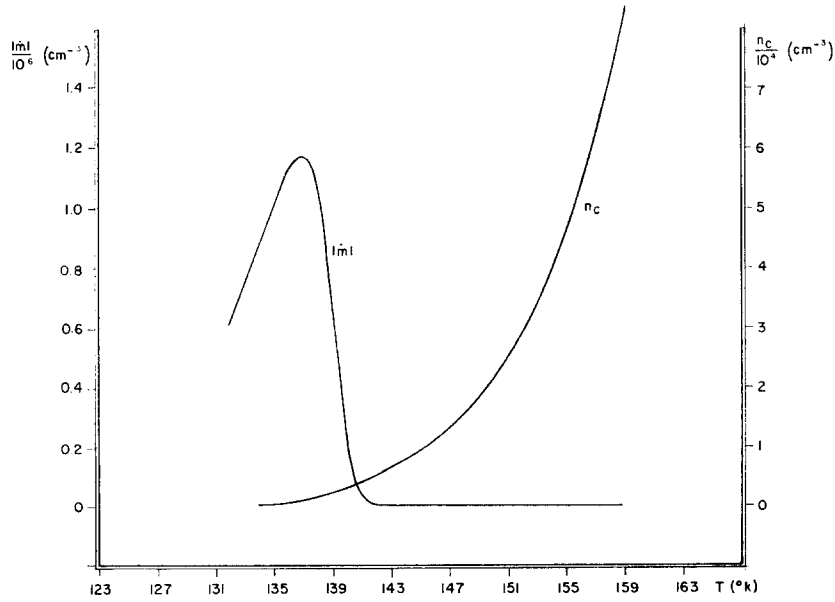

FIG. 4. Calculated curves of n_c and $|\dot{m}|$. $A = 5 \times 10^{-4}$ cm^3 sec^{-1}, $B = 10^{-7}$ cm^3 sec^{-1}, $m_0 = 10^7$ cm^{-3}, $n_0 = 10^8$ cm^{-3}, $N = 10^{10}$ cm^{-3}, $P_0 = 10^{10}$ sec^{-1}, $E = 0.316$ev, $\beta = 1K$ sec^{-1}, $n_{c0} = 8.5$ cm^{-3}, $T_0 = 120K$.

when m changes only slightly during the process, as is the case in Fig. 1. The broad n_c peak is also to be noted; this effect was described by Saunders [11].

Figure 3 shows the two peaks for $m_0 = n_0$ and $A = 3 \times 10^{-5}\,\text{cm}^3\,\text{sec}^{-1}$ and $B = 10^{-7}\,\text{cm}^3\,\text{sec}^{-1}$. The parameters were chosen such that the TL peak would be neither of first nor of second order kinetics. The resulting curve is characterized by $\mu_g = 0.468$. This value may correspond to an effective order of kinetics, l, [12] which is between 1 and 2 (about 1.4 in this special case).

Figure 4 gives the TL peak and the n_c curve for $A = 5 \times 10^{-4}\,\text{cm}^3\,\text{sec}^{-1}$, $B = 10^{-7}\,\text{cm}^3\,\text{sec}^{-1}$, $m_0 = 10^7\,\text{cm}^{-3}$ and $n_0 = 10^8\,\text{cm}^{-3}$. This figure has two peculiarities: the n_c curve is steadily increasing exponentially in the range of interest as found experimentally for semiconducting diamonds [13] and discussed for certain cases [4], and the μ_g value found for this TL peak is extremely small, about 0.308 which does not correspond to any reasonable effective order of kinetics. Such peaks, which are rather rarely found in experiments, were mentioned by Halperin and Braner [1] who showed that such an effect should be expected when there is a shortage of luminescence centers (namely, $m_0 < n_0$). It is to be mentioned, again, that as compared to the peaks of Halperin and Braner, the curves are found presently without the assumption $|\dot{n}_c| \ll |\dot{n}|$.

TABLE I

Representative Values for Checking the Validity of the Condition $|\dot{n}_c| \ll |\dot{n}|$

$T(K)$	$\dot{m}(T)/\dot{m}(T_m)$	$\lvert\dot{n}_c(T)/\dot{m}(T)\rvert$	$\lvert\dot{n}_c(T)/\dot{n}(T)\rvert$	$T(K)$	$\dot{m}(T)/\dot{m}(T_m)$	$\lvert\dot{n}_c(T)/\dot{m}(T)\rvert$	$\lvert\dot{n}_c(T)/\dot{n}(T\rvert)$
	Curve 1				Curve 3		
90	8.3×10^{-4}	5.0×10^{-5}	5.0×10^{-5}	110	4.3×10^{-4}	1.7×10^{-4}	1.7×10^{-4}
95	7.1×10^{-3}	4.0×10^{-4}	4.0×10^{-4}	120	6.9×10^{-3}	8.5×10^{-5}	8.5×10^{-5}
100	4.9×10^{-2}	3.6×10^{-4}	3.6×10^{-4}	130	7.1×10^{-2}	7.3×10^{-5}	7.3×10^{-5}
105	2.5×10^{-1}	3.0×10^{-4}	3.0×10^{-4}	140	4.5×10^{-1}	6.9×10^{-5}	6.9×10^{-5}
110	8.5×10^{-1}	1.5×10^{-4}	1.5×10^{-4}	150	9.9×10^{-1}	8.4×10^{-5}	8.4×10^{-5}
115	6.0×10^{-1}	4.0×10^{-4}	4.0×10^{-4}	160	2.5×10^{-1}	6.4×10^{-5}	6.4×10^{-5}
				170	3.6×10^{-2}	5.5×10^{-4}	5.5×10^{-4}
				180	7.4×10^{-3}	1.6×10^{-3}	1.6×10^{-3}
	Curve 2				Curve 4		
140	1.3×10^{-2}	5.0×10^{-2}	4.8×10^{-2}	120	3.6×10^{-2}	1.0×10^{-4}	1.0×10^{-4}
150	7.2×10^{-2}	1.6×10^{-2}	1.6×10^{-2}	125	1.2×10^{-1}	5.1×10^{-5}	5.1×10^{-5}
160	3.0×10^{-1}	1.4×10^{-2}	1.4×10^{-2}	130	3.6×10^{-1}	6.1×10^{-5}	6.1×10^{-5}
170	7.8×10^{-1}	1.2×10^{-2}	1.2×10^{-2}	135	8.6×10^{-1}	1.4×10^{-4}	1.4×10^{-4}
180	9.8×10^{-1}	9.9×10^{-3}	9.8×10^{-3}	140	1.9×10^{-1}	4.5×10^{-3}	4.5×10^{-3}
190	6.0×10^{-1}	5.6×10^{-3}	5.5×10^{-3}	145	1.5×10^{-7}	8.7×10^{8}	1.0
200	2.6×10^{-1}	5.1×10^{-3}	5.1×10^{-3}	150	1.5×10^{-22}	1.9×10^{19}	1.0
210	1.0×10^{-1}	3.4×10^{-2}	3.6×10^{-2}	155	1.9×10^{-57}	3.2×10^{54}	1.0
220	4.1×10^{-2}	8.5×10^{-2}	9.3×10^{-2}				

TABLE II

Given Sets of Parameters and Calculated Values of the Peaks' Temperatures and Geometrical Factors

No.	$m_0(\text{cm}^{-3})$	$n_0(\text{cm}^{-3})$	$n_{c0}(\text{cm}^{-3})$	$N(cm^{-3})$	$A(\text{cm}^3\text{sec}^{-1})$	$B(\text{cm}^3\ \text{sec}^{-1})$	$P_0(\text{sec}^{-1})$	$E(\text{eV})$	$T_m(K)$	$T_{nc}-T_m$	$\mu_g(TL)$
1	10^7	10^8	3.18	10^{10}	1.5×10^{-3}	10^{-7}	10^{10}	0.316	136.5	—[a]	0.234
2	10^7	10^8	4.62	10^{10}	10^{-3}	10^{-7}	10^{10}	0.316	136.6	—[a]	0.256
3	10^7	10^8	8.48	10^{10}	5.0×10^{-4}	10^{-7}	10^{10}	0.316	136.8	—[a]	0.308
4	10^{10}	10^8	0.18	10^{10}	10^{-5}	10^{-7}	10^{14}	0.316	109.9	0	0.416
5	10^{10}	10^8	9.45	10^{10}	10^{-7}	10^{-7}	10^{14}	0.633	219.8	0	0.416
6	10^{10}	10^8	9.45	10^{10}	10^{-7}	10^{-7}	10^{14}	0.316	112.1	0	0.418
7	10^8	10^8	0.50	10^{10}	10^{-3}	10^{-7}	10^{10}	0.316	148.1	8.9	0.420
8	10^8	10^8	0.02	10^{10}	5.0×10^{-5}	10^{-7}	10^{10}	0.316	148.6	8.29	0.454
9	10^8	10^8	0.79	10^{10}	3.0×10^{-5}	10^{-7}	10^{10}	0.316	149.1	8.91	0.468
10	10^8	10^8	4025	10^{10}	10^{-7}	10^{-7}	10^{10}	0.316	177.8	19.58	0.525
11	10^8	10^8	406	10^{10}	10^{-7}	10^{-5}	10^{10}	0.316	222.3	28.49	0.532

[a] $T_{nc} \gg T_m$.

Table I gives some results of the test for the validity of the condition $|\dot{n}_c| \ll |\dot{n}|$ usually assumed in TL theory for the four cases given in Figs. (1–4). The values of $\dot{m}(T)/\dot{m}(T_m)$ in column 2 show the position of the various TL points as compared to the maximum. The corresponding values of columns 3 and 4 are equal as long as the above-mentioned condition is fulfilled; the values of $|\dot{n}_c(T)/\dot{m}(T)|$ are small in these ranges. It is clearly seen that the condition is not satisfied any more in the case related to Fig. (4) at temperatures above the maximum.

Table II summarizes the results found for various sets of given parameters including those shown in Figs. (1–4) (Nos. 6, 10, 9 and 3 in the table, respectively). The table is arranged according to the increasing values of μ_g, namely, starting from the case of "shortage of centers" through first order kinetics, "intermediate" order and second order TL peaks.

Calculation of Activation Energies

Having developed a simulating model for TL and TSC phenomena, it is easy to evaluate the theoretical accuracy of methods for calculating crystal parameters from TL and TSC curves. We were interested in certain methods for calculating the activation energy E.

These methods, using temperature of the peak maximum T_m and the half intensity temperatures T_1 and T_2 were developed under the assumption that the peak has a definite order of kinetics. The order was assumed to be first or second in various methods, and any order l between 0.7 and 2.5 when interpolation (and extrapolation) between first and second order cases was applied [12]. In order to check the methods, we applied them to the general glow peaks calculated by the present method in order to find whether an effective value of l can be found such that the solution of $-\dot{n} = s' \exp(-E/kT)\, n^l$ would be close enough to our glow curve so that the methods for finding E from the latter can be used for the former.

The three equations given by Chen [12] are

$$E_\tau = [1.51 + 3.0(\mu_g - 0.42)]\, kT_m^2/\tau - [1.58 + 4.2(\mu_g - 0.42)]\, 2kT_m\,, \quad (20)$$

$$E_\delta = [0.976 + 7.3(\mu_g - 0.42)]\, kT_m^2/\delta, \quad (21)$$

$$E_\omega = [2.52 + 10.2(\mu_g - 0.42)]\, kT_m^2/\omega - 2kT_m\,, \quad (22)$$

where τ is defined by $\tau = T_m - T_1$. Table III gives the found values of E_τ, E_δ, E_ω, μ_g and T_m for the 10 first curves given in Table II. Apart from the rare first three cases which have "abnormal" shape [1], all the methods give rather good values, E_τ being the best. As could be expected from an interpolation method, the values are excellent where the circumstances are such that the peaks are close to be of first or second order. For E_τ, however, the deviations from the correct

TABLE III
Activation Energies by Various Methods

No.	E_0	E_τ	E_δ	E_ω	μ_g	T_m
1	0.316	0.311	−0.437	0.141	0.234	136.5
2	0.316	0.318	−0.215	0.186	0.256	136.6
3	0.316	0.342	0.114	0.276	0.308	136.8
4	0.316	0.315	0.306	0.314	0.416	109.9
5	0.633	0.630	0.631	0.628	0.416	219.8
6	0.316	0.316	0.309	0.316	0.418	112.1
7	0.316	0.315	0.317	0.318	0.420	148.1
8	0.316	0.323	0.341	0.336	0.454	148.6
9	0.316	0.331	0.344	0.339	0.468	149.1
10	0.316	0.314	0.325	0.321	0.525	177.8

value do not exceed 5% even for intermediate order cases. This is usually comparable to the possible experimental error. Even for the three first cases, the E_τ method gives good results since the "abnormality" of the peaks is demonstrated mainly in the high temperature portion.

Summary and Conclusions

The three simultaneous differential equations governing the processes of thermoluminescence and thermally stimulated conductivity have been solved, for the first time, to the best of our knowledge, with no additional a priori assumptions made about the functions m, n and n_c. The results are used for examining the assumptions made by previous investigators showing that those assumptions were usually rather good. Methods for evaluating the activation energy E were applied to the computed peaks, showing that at least one of these methods is very good for evaluating activation energies. It was seen, however, that the peaks' shapes are less sensitive to the other parameters (see also [6, 7]) and therefore the evaluation of these parameters (A, B, P_0, etc.) would be much harder using only three measured values like T_1, T_m and T_2. More experimental points should be used, as well as information on the corresponding TSC curve. An investigation along these lines is under way now, and the results seem to be rather promising.

As mentioned above, the kinetics order depends on the ratio between Am and $B(N-n)$. This "order" will remain constant if $Am > B(N-n)$ or $Am < B(N-n)$ is true throughout the peak. This inequality can, however, change direction during the process so that the term "kinetics order" may become meaningless. This explains the "abnormality" of the first three peaks in Tables I and II (see also [1, 5]).

Note. While considering some corrections in the manuscript as required by the referees (October 1971), we learnt of a paper describing the numerical solution of the equations governing the thermally stimulated processes (P. Kelly, M. J. Laubitz and P. Bräunlich, *Phys. Rev. B* 4 (1971, 1960–68)). The computational method used in that paper was, however, entirely different and so were the chosen ranges of the parameters and some of the conclusions.

References

1. A. Halperin and A. A. Braner, *Phys. Rev.* **117** (1960), 408.
2. G. A. Dussel and R. H. Bube, *Phys. Rev.* **155** (1967), 764.
3. I. J. Saunders, *J. Phys. C* **2** (1969), 2181.
4. P. L. Land, *J. Phys. Chem. Solids* **30** (1969), 1681, 1693.
5. D. De-Muer, *Physica* **48** (1970), 1.
6. P. Kelly and P. Bräunlich, *Phys. Rev. B* **1** (1970), 1587, 1596.
7. P. Kelly and P. Bräunlich, *Phys. Rev. B* **3** (1971), 2090.
8. Y. R. Barkley, A Runge-Kutta for all Seasons. The University of Wisconsin, Madison, Wisconsin, AD-642910 (1966).
9. R. Chen, *J. Appl. Phys.* **40** (1969), 570.
10. R. Chen, *J. Appl. Phys.* **42** (1971), 5899.
11. I. J. Saunders, *Brit. J. Appl. Phys.* **18** (1967), 1219.
12. R. Chen, *J. Electrochem. Soc.* **116** (1969), 1254.
13. A. Halperin and R. Chen, *Phys. Rev.* **148** (1966), 839.